

## Effect of Ag<sup>+</sup> ion Concentration on the Reaction Kinetics and Shape of Nanoparticles Synthesised by Green Chemical Approach

S.S. Kalyan Kamal\*, J. Vimala, P.K. Sahoo, P. Ghosal, and L. Durai

Defence Metallurgical Research Laboratory, Hyderabad - 500 058, India

\*Email: kalyanchem@dmrl.drdo.in

### ABSTRACT

The effect of varying Ag<sup>+</sup> ion concentration on the green chemical reaction with a fixed tea aliquot concentration has been studied in detail with the help of UV-visible absorption spectra. With increase in the concentration of Ag<sup>+</sup> solution the position of surface plasmon band systematically increased from 435 nm – 450 nm. The reaction followed first order kinetics and the rate of reaction increased in a linear fashion with  $k = 3.54 \times 10^{-4} \text{ min}^{-1}$  for 0.5 mL to  $k = 1.86 \times 10^{-3} \text{ min}^{-1}$  for 3.0 mL Ag<sup>+</sup> solution. X-ray diffraction patterns showed an enhanced (200) reflection for 3.0 mL Ag sample. The shape of Ag nanoparticles could be effectively tuned from spherical to cuboid with increase in silver content as evidenced from scanning electron and transmission electron micrographs. The average particle size of Ag NPs increased from 25 nm to 55 nm with increase in the Ag<sup>+</sup> content of the reaction.

**Keywords:** Silver nanocubes, green chemical synthesis, UV-vis absorption spectra, reaction kinetics

### 1. INTRODUCTION

Green chemical synthesis of nanoparticles (NPs) has become prominent due to its environmental friendliness, ease of operation and good biocompatibility. Special interest has been laid on biogenic routes for production of silver (Ag) NPs due to their potential applications in the fields of catalysis, non linear optics and biology<sup>1-5</sup>. Easily tunable surface plasmon resonance (SPR) band of Ag NPs in the UV-vis and NIR region makes it a sought after biomaterial. Controlling the size and shape of Ag NPs is not only of academic interest but has a bearing on many properties such as catalytical activity and optical properties<sup>6,7</sup>. Therefore a plethora of environmental friendly routes have been explored for synthesis of Ag NPs, which includes the use of both plant products and cell cultures<sup>4,5,8</sup>. The former has been a widely adopted process as it does not require cumbersome maintenance of cell cultures.

Various plant products that have been explored for the synthesis of Ag NPs thus far includes *Zingiber officinale*, *Embilica officinalis*, *Acacia oolotica*, *Cochlospermum gossypium*, *Eucalyptus macrocarpa*, *Stevia rebaudiana*, *Azadirachta Indica*, and *Camellia sinensis* (tea) leaves<sup>2,4,5,9-12</sup>. Tea leaf extract is a rich source of polyphenolic compounds, which performs the dual role of reducing and stabilizing agent. Additionally it imparts the NPs with synergistic health benefits of protection against heart diseases, cancer and neurotoxins<sup>13,14</sup>. Though a lot of emphasis has been laid on the development of green chemical approaches, very little work has been carried out in the direction of understanding the kinetics of these reactions<sup>8,15,16</sup>. Determining the kinetic parameters of biological approaches is an important aspect which leads to better

understanding of the reaction for their scale up and long term sustainability of the process at industrial scale. The kinetics also plays an important role on the size and shape of NPs, which ultimately have a pronounced effect on their functional properties such as catalytical and optical properties.

A complete green chemical route for the synthesis of Ag NPs in the form of spheres and cubes using tea leaf extract is reported. The kinetics of Ag<sup>+</sup> → Ag<sup>0</sup> green chemical reaction was studied in detail with the help of UV-vis spectra. The role of Ag<sup>+</sup> ion concentration on the rate of reaction and shape of Ag NPs is discussed in detail.

### 2. EXPERIMENTAL WORK

To obtain 5.8 x 10<sup>-3</sup> M Ag<sup>+</sup> solution 0.1 g of silver nitrate (AgNO<sub>3</sub>, 99.9% pure) obtained from Alfa Aesar Laboratories, Germany, was dissolved in 100 mL of ultra high pure water with a resistivity of 18.2 MΩcm. Tea broth was prepared by dissolving 1.0 g of tea granules in 100 mL of water. The contents were left overnight to extract the polyphenolic compounds into the solvent. A reddish brown tea aliquot was collected after separation of undissolved matter through filtration and centrifugation. In order to study the effect of Ag<sup>+</sup> ion concentration on the chemical reaction with tea aliquot, four experiments were carried out with varying contents of Ag<sup>+</sup> solution (0.5 mL, 1 mL, 2 mL, and 3 mL) against a fixed volume of tea solution (3 mL). Net contents of the reaction vials were topped up with water to obtain a fixed volume of 10 mL as shown in Table. 1. The vials were tightly capped to prevent evaporation losses during the reaction process.

The reduction reaction of Ag<sup>+</sup> → Ag<sup>0</sup> was followed through absorption spectra recorded at periodic intervals of 15 min using a T90+ UV-vis spectrometer. In order to obtain the

**Table 1.** Experimental parameters adopted for synthesis of Ag-NPs along with their chemical composition

Expt	$Ag^+$ ( $5.8 \times 10^{-3}$ M) (mL)	Tea liqout (mL)	$H_2O$ (mL)	Chemical Composition (wt%)		
				Ag	C	O
(a)	0.5	3.0	6.5	97.9 (0.5)	1.74 (0.07)	0.29 (0.03)
(b)	1.0	3.0	6.0	98.8 (0.5)	1.05 (0.07)	0.15 (0.02)
(c)	2.0	3.0	5.0	99.0 (0.5)	0.86 (0.07)	0.12 (0.02)
(d)	3.0	3.0	4.0	99.1 (0.5)	0.83 (0.07)	0.13 (0.02)

chemical composition of the as-prepared NPs, the solutions were centrifuged at 5000 RPM followed by thorough washing with water several times to remove any unreacted substances before carrying out the analysis. Three different techniques namely inductively coupled plasma optical emission spectrometer (ICPOES) model JY Ultima, Leco carbon and sulphur analyser model CS-444 and Leco oxygen and nitrogen analyser model TC-600 were used for obtaining the chemical constituents. To study the effective capping of bio-molecules on the Ag NPs surface a Tensor 27 Fourier transform infrared spectrometer (FTIR) was used. Crystal structure of as-synthesised Ag NPs was obtained using a Philips-PW3020 X-ray diffractometer (XRD). Microstructural characterisation of as-synthesised Ag NPs was carried out with the help of scanning electron microscope (SEM) and transmission electron microscope (TEM- Philips,

TECHNAI FE 12). Ag NPs were redispersed in water using ultrasonication and drop coated onto a carbon tape and carbon coated 2 mm copper grid to obtain SEM and TEM micrographs, respectively.

### 3. RESULTS AND DISCUSSION

A chemical reaction between  $Ag^+$  ions and tea polyphenols was followed both visually and through UV-vis absorption spectra. Change in colour of reaction medium from pale yellow to dark yellow indicates the reduction of  $Ag^+$  ions and formation of Ag NPs. Fig. 1 shows the UV-vis absorption spectra obtained wrt time for 240 min at an interval of 15 min upon reaction of  $Ag^+$  ions (a) 0.5 mL, (b) 1.0 mL, (c) 2.0 mL, and (d)

3.0 mL with a fixed volume of tea aliquot (3 mL). As observed from Fig. 1(a) - 1(d) a characteristic surface plasmon resonance (SPR) band exists in the region of 435 nm - 450 nm in all the spectra indicating the formation of Ag NPs. From Fig. 1(a) it could be observed that  $Ag^+ \rightarrow Ag^0$  is a slow reaction, which takes 4 h to complete but starts as early as 15 min. The position of SPR band red-shifts systematically from 435 nm to 450 nm with increase in  $Ag^+$  concentration from 0.5 mL to 3.0 mL as observed in Fig. 1(a)-(d) and Table 2. This suggests that the particle size of Ag NPs increases with increase of silver content against a fixed concentration of tea extract.

Kinetics of the  $Ag^+ \rightarrow Ag^0$  reaction with different  $Ag^+$  ion concentrations were studied by plotting the absorbance intensity vs. reaction time graphs as shown in Fig. 2(a). From the Fig. 2 could be observed that the reaction follows a linear

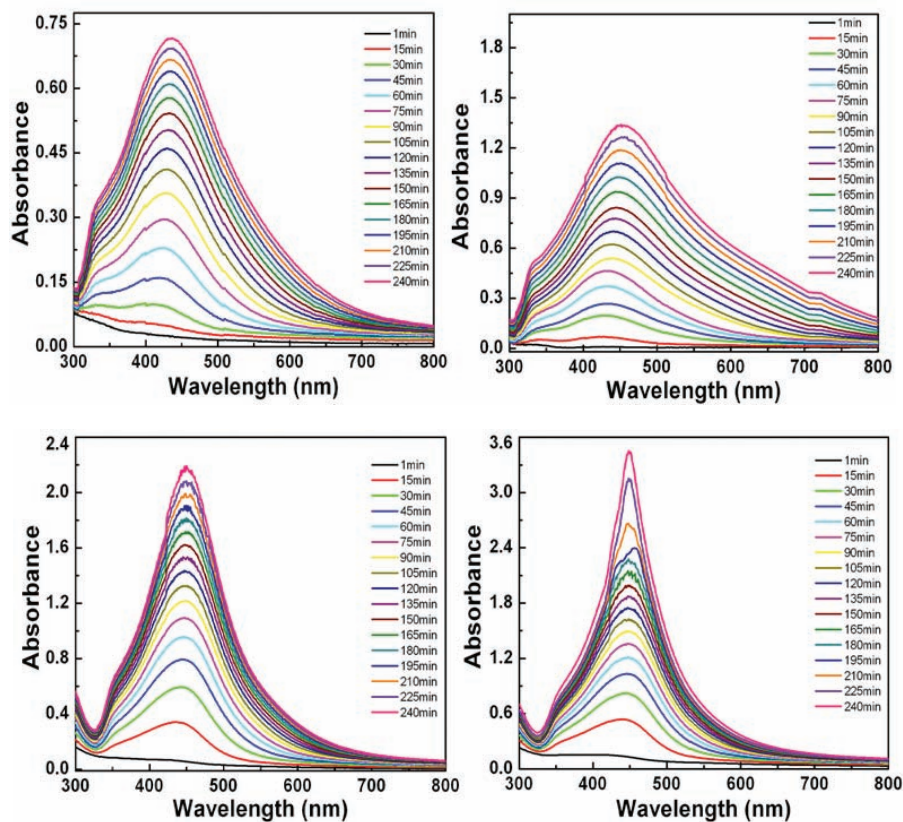


**Figure 1.** UV-vis absorption spectra with respect to time for 240 min at an interval of 15 min upon reaction of  $Ag^+$  ions (a) 0.5 mL, (b) 1.0 mL, (c) 2.0 mL, and (d) 3.0 mL with a fixed volume (3 mL) of tea aliquot.

**Table 2. Average position of surface plasmon resonance band, ratio of  $I_{(111)}/I_{(200)}$  peak, particle shape and size obtained from samples (a-d) under different experimental conditions**

Sample	SPR band (nm)	Ratio of $I_{(111)}/I_{(200)}$	Particle shape	Average particle size (nm)
(a)	435	4.95	Spherical	23
(b)	445	3.45	Spherical	36
(c)	448	2.77	Spherical + Cubical	45
(d)	452	0.51	Cubical	58

trend and can be fit to a first order rate equation given by

$$A_t = A_\infty (1 - e^{-kt})$$

where  $A_t$  and  $A_\infty$  represent the absorbencies recorded at a given time ( $t$ ) and at a very long time respectively,  $k$  represents the rate constant corresponding to a first-order reaction. To obtain the rate of the reaction, the above equation can be modified as,

$$-\ln(1-a) = kt$$

where  $a = A/A_\infty$ , the reaction rate plots were obtained by plotting the  $-\ln(1-a)$  as a function of time and are shown in Fig. 2(b). At all the four given Ag concentrations they exhibit a linear behavior, except for a slight deviation in sample (d) above 180 min. The reaction rates were determined using the above plots,  $k = 3.54 \times 10^{-4} \text{ min}^{-1}$  for 0.5 mL,  $k = 5.85 \times 10^{-4} \text{ min}^{-1}$  for 1.0 mL,  $k = 1.39 \times 10^{-3} \text{ min}^{-1}$  for 2.0 mL, and  $k = 1.86 \times 10^{-3} \text{ min}^{-1}$  for 3.0 mL. These results suggest that with the increase in  $\text{Ag}^+$  content from 0.5 mL to 3.0 mL the rate of the reaction increases systematically and follow a linear trend as shown in Fig. 3.

Chemical compositions of the as-prepared Ag NPs are shown in Table 1. along with their standard deviation given in parenthesis. It could be observed that two minor constituents in the form of C and O are present along with the major content Ag in all the samples. With increase in  $\text{Ag}^+$  content from experiments (a) - (d) the Ag content in the final product increases and the corresponding C (1.74 % to 0.83 %) and O (0.29 % to 0.13 %) content decreases in the samples systematically. Decrease in the trace elements (C and O) with increasing Ag content suggests that the availability of surfactant to cap the Ag NPs decreases.

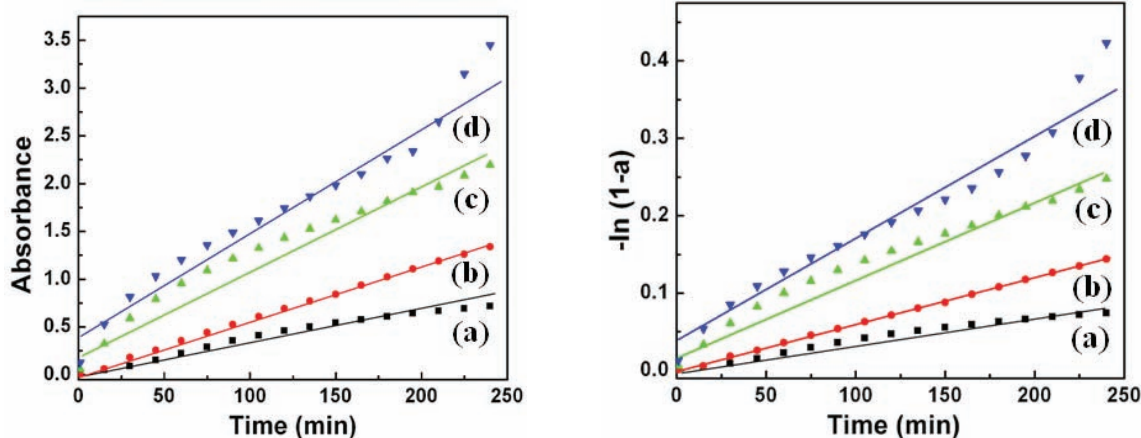


**Figure 2. (A) UV-vis absorbance intensity at  $\lambda_{\text{max}}$  vs. reaction time plots and their corresponding kinetics plots (B) obtained from different  $\text{Ag}^+$  ion concentrations (a) 0.5 mL, (b) 1.0 mL, (c) 2.0 mL, and (d) 3.0 mL.**

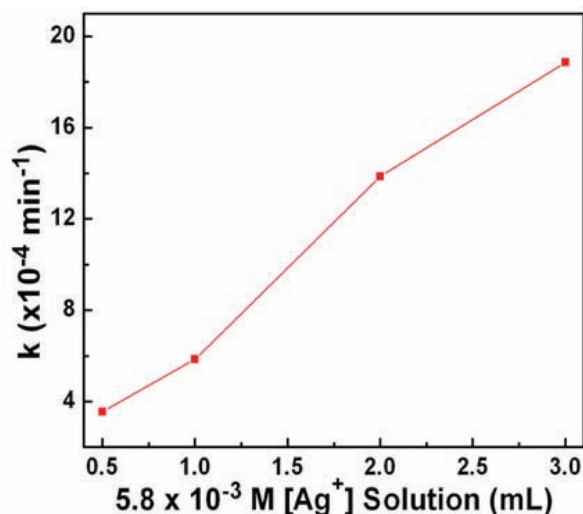


**Figure 3. Rate of reaction vs. Ag concentration plot obtained upon reaction with tea extract for 4 h.**

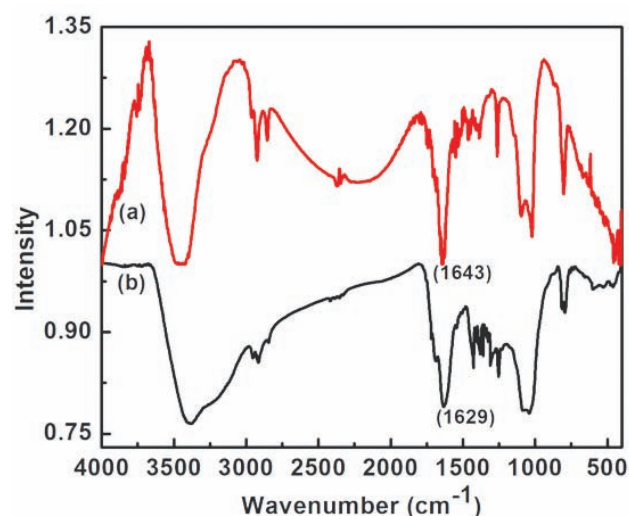


**Figure 4. FTIR spectra of virgin tea aliquot and Ag nanoparticles protected by tea polyphenols.**

The nature of interaction between the tea extract and Ag NPs was studied with the help of FTIR spectra. Fig. 4 shows the FTIR spectra of (a) un-reacted tea extract, and (b) colloidal solution of Ag NPs obtained after the reaction. From Fig. 4(a) it could be observed that the un-reacted tea extract consists of a broad peak at  $3400\text{ cm}^{-1}$  corresponding to the O-H stretch and the peaks at  $2850\text{ cm}^{-1}$  could be attributed to the  $sp^2$  C-H stretch. Peak at  $1643\text{ cm}^{-1}$  could be attributed to the C=O stretch of the acid groups present in thearubigins and small peaks present at  $840\text{ cm}^{-1}$  and  $550\text{ cm}^{-1}$  confirms the presence of aromatic substituted rings. Except for a slight shift in the C=O stretch from  $1643\text{ cm}^{-1}$  to  $1629\text{ cm}^{-1}$  rest of the peaks remain unchanged in the spectra obtained from that of Ag NPs after the reaction with tea extract as shown in Fig. 4(b). The slight red shift in the carbonyl frequency by  $14\text{ cm}^{-1}$  indicates a weak coordination between the carbonyl group and Ag NPs and thus proves that the Ag NPs are protected by the natural polyphenols present in tea.

Figures 5(a)-(d) shows the XRD patterns of Ag nanopowders obtained from various samples (a)-(d). A typical XRD pattern of a face centered cubic (fcc) structure was obtained from all the four samples, consisting of three distinct peaks at corresponding  $2\theta$  values of  $38.29^\circ$ ,  $44.63^\circ$  and  $65.71^\circ$ . The discernible peaks could be indexed to (111), (200) and (220) planes of a cubic unit cell, corresponding to an fcc structure of Ag (JCPDS card No. 87-0720). With a lattice parameter  $a = 0.4064\text{ nm}$ , i.e., smaller relative to the bulk value  $0.4077\text{ nm}$ . The XRD data upon normalisation show a standard pattern for samples (a) - (c) with normalised major intensity peak  $I_p = 100$  for the (111) plane at a  $d$  spacing of  $0.2345\text{ nm}$ . In case of sample (d) the pattern changes drastically wherein the major intensity peak arises from the (200) plane at a  $d$  spacing of  $0.2043\text{ nm}$ . This peculiar behavior of enhanced intensity of the (200) plane in sample (d) over samples (a) - (c) could be explained by the fact that there could be a possible change in the particle shape from spherical (in samples (a)-(c)) to cuboid (in sample (d)). This conclusion is based on the fact that most of the nanocubes tend to align themselves flat on the substrate

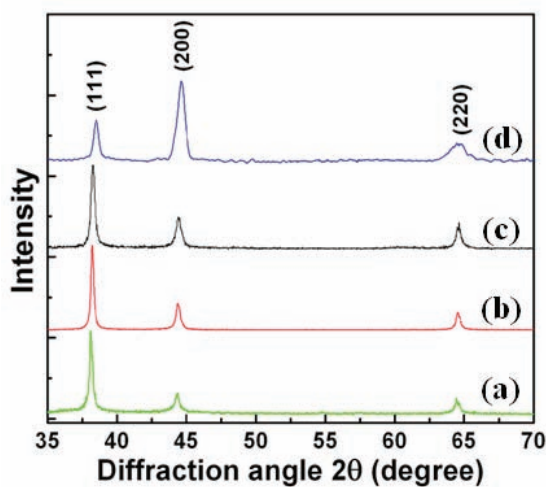


Figure 5. X-ray diffraction patterns of Ag nanoparticles obtained from different samples (a) 0.5 mL, (b) 1.0 mL, (c) 2.0 mL, and (d) 3.0 mL  $Ag^+$  solutions after 4 h of reaction with tea aliquot.

with their (200) planes parallel to the substrate, leading to an enhanced intensity from (200) plane over the (111) Bragg reflection<sup>6</sup>. The ratio of  $I_{(111)}/I_{(200)}$  peak decreases with increase in Ag concentration from samples (a-d) as shown in Table 2. This suggests that with increasing the  $Ag^+$  content against a fixed concentration of tea aliquot the sphericity of the Ag NPs slowly distorts to form nanocubes.

To determine the particle size and shape of Ag NPs SEM and TEM micrographs were analysed. Figs. 6(a) - 6(d) shows the SEM micrographs obtained from samples (a)-(d), which reveals that the particle shape is predominantly spherical in case of samples (a) - (c) and average size of the Ag NPs increases from 25 nm to 35 nm, and 40 nm for samples (a), (b), and (c), respectively. In case of sample (d) the SEM micrograph shows cuboidal shaped Ag NPs with an average size of 55 nm. This result is in good agreement with the XRD pattern observed in Fig. 5(d), wherein the major intensity peak was from (200) plane. Fig. 6(e) shows a typical energy dispersive X-ray spectrum obtained from sample (d), showing three peaks for Ag, C, and O. The presence of C and O peaks suggest that the polyphenolic compounds have formed a stable surface coating over the Ag NPs thus effectively restricting the particle size to nano-regime and corroborates well with the chemical composition and FTIR data. However, a high intensity peak for C cannot be completely attributed to the organic moieties

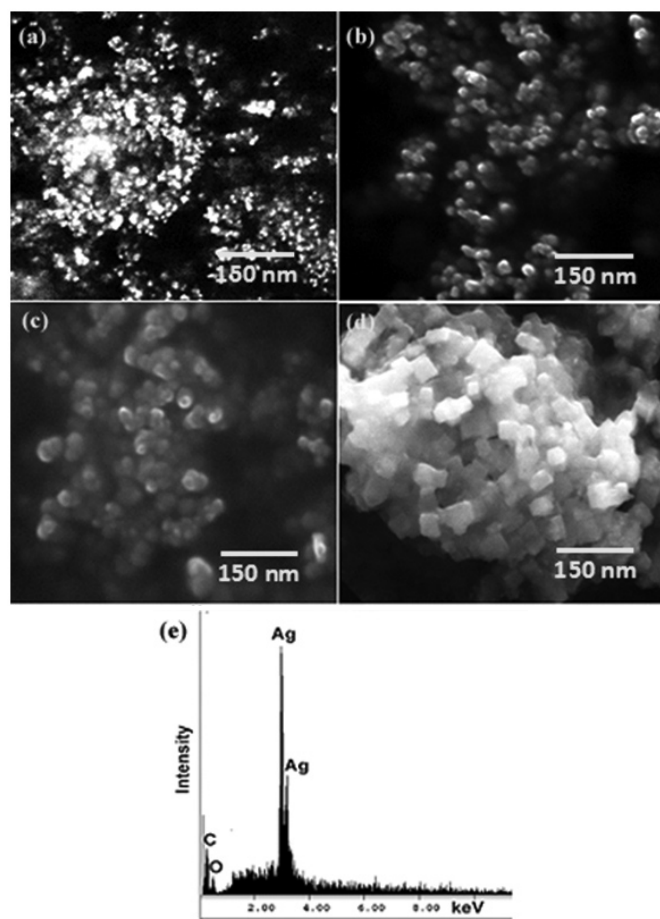
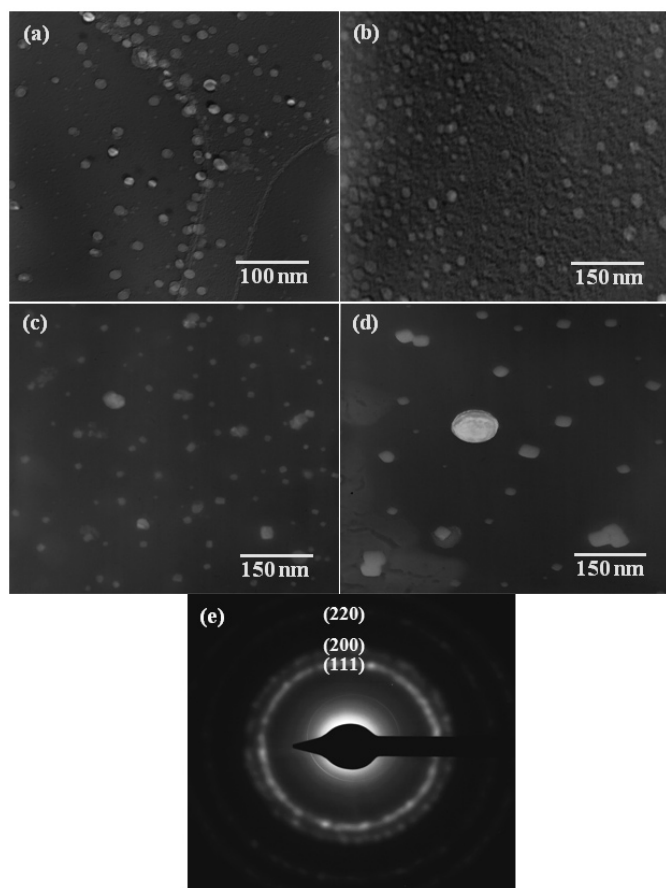


Figure 6. SEM micrographs of Ag nanoparticles obtained from different samples a) 0.5 mL, (b) 1.0 mL, (c) 2.0 mL, and (d) 3.0 mL  $Ag^+$  solutions after 4 h of reaction with tea aliquot.



**Figure 7.** TEM micrographs of Ag nanoparticles obtained from different samples a) 0.5 mL, (b) 1.0 mL, (c) 2.0 mL, and (d) 3.0 mL  $\text{Ag}^+$  solutions after 4 h of reaction with tea aliquot.

of tea extract alone but to the carbon tape used for holding the sample.

To carry out detailed microstructural characterisation of the samples TEM micrographs were obtained from samples (a)-(d) as shown in Fig. 7. The TEM results are in good agreement with the SEM results and depict spherical shaped Ag NPs for samples (a)-(c) and nanocuboids for sample (d). Figure 7 (e) shows the selected area electron diffraction pattern obtained from sample (d), which shows three concentric rings at  $d$  spacing of 0.2346 nm, 0.2041 nm, and 0.1439 nm corresponding to (111), (200), and (220) lattice reflections respectively, which are concomitant with the XRD patterns. The average particle size of Ag NPs increases with increase in the Ag content of the sample from 23 nm to 36 nm to 45 nm and 58 nm for samples (a), (b), (c), and (d) respectively and are in good agreement with the UV-vis absorption spectra, wherein the SPR peak red shifts to higher wavelengths systematically from samples (a) - (d). This systematic increase in particle size could be explained by the fact that in all the experiments the tea aliquot is kept constant but the Ag content is increased, which suggests that at lower Ag content (sample (a)) the polyphenolic compounds effectively control the size to 25 nm. As the Ag content increases the net availability of the organic moieties to cap the Ag NPs reduces therefore leading to an increased particle size. Another interesting observation is that the shapes of the Ag NPs vary from nanospheres in samples (a) and (b)

to a mixture of nanospheres and nanocubes in sample (c) to majority > 95 per cent nanocubes in sample (d) with increased Ag content.

#### 4. CONCLUSIONS

A simple, reproducible, quick, cost effective and complete green chemical route for the synthesis of shape anisotropic Ag NPs in the form of nanospheres and nanocubes has been developed. The detailed study on role of initial  $\text{Ag}^+$  ion concentration on the rate of the reaction has been established through UV-vis absorption spectra and it shows a systematic linear behavior. Shape of Ag NPs could be easily tuned from spherical to nanocubes by simply changing the  $\text{Ag}^+$  content in the reaction rather than using conventional heterogeneous nucleation routes, which are time consuming and cumbersome.

#### REFERENCES

1. Raja, S.; Ramesh, V. & Thivaharan, V. Green biosynthesis of silver nanoparticles using *Calliandra haematocephala* leaf extract, their antibacterial activity and hydrogen peroxide sensing capability. *Arab. J. Chem.* 2015. doi:10.1016/j.arabjc.2015.06.023
2. White, G.V.; Kerscher, P.; Brown, R.M.; Morella, J.D.; McAllister, W.; Dean, D. & Kitchens, C.L. Green synthesis of robust, biocompatible silver nanoparticles using garlic extract. *J. Nanomaterials*, 2012, **730746**, 1-12. doi.org/10.1155/2012/730746
3. Cox, S.G.; Cullingworth, L. & Rode, H. Treatment of paediatric burns with a nanocrystalline silver dressing compared with standard wound care in a burns unit: a cost analysis. *South Afr. Med. J.*, 2011, **101** (10), 728-731.
4. Balaprasad, A.; Chinmay, D.; Ahmad, A. & Sastry, M. Biosynthesis of gold and silver nanoparticles using *Emblca Officinalis* fruit extract, their phase transfer and transmetallation in an organic solution. *J. Nanosci. Nanotech.*, 2005, **5**, 1665-1671. doi: 10.1166/jnn.2005.184
5. Shankar, S.S.; Rai, A.; Ahmad, A.; Pasricha, R. & Sastry, M. Rapid synthesis of Au, Ag and bimetallic Au core-Ag shell nanoparticles using Neem (*Azadirachta Indica*) leaf broth. *J. Coll. Interface Sci.*, 2004, **275**, 496-502. doi:10.1016/j.jcis.2004.03.003
6. Bansal, V.; Li, V.; O'Mullane, A.P. & Bhargava, S.K. Shape dependent electrocatalytic behaviour of silver nanoparticles. *Cryst. Eng. Comm.* 2010, **12**, 4280-4286. doi: 10.1039/C0CE00215A
7. González, A.L. & Noguez, C. Influence of morphology on the optical properties of metal nanoparticles. *J. Comp. Theor. Nanosc.*, 2007, **4**(2), 231-238. doi:10.1166/jctn.2007.005
8. Nair, P.P. Kinetics of biosynthesis of silver nanoparticles using *Fusarium oxysporum*. *Cur. Trends Techn. Sc.*, 2012, **1** (1), 47-52.
9. Poinern, G.E.J.; Chapman, P.; Shah, M. & Fawcett, D. Green biosynthesis of silver nanocubes using the leaf extracts from *Eucalyptus macrocarpa*. *Nano Bulletin*,

- 2013, **2**(1), 130101(1-7).
10. Varshneya, R.; Bhadauriaa, S. & Gaur, M.S. Biogenic synthesis of silver nanocubes and nanorods using sundried *Stevia rebaudiana* leaves. *Adv. Mater. Lett.*, 2010, **1**(3), 232-237. doi:10.5185/amlett.2010.9155
  11. Vinod, V.T.P.; Saravanan, P.; Sreedhar, B.; Devi, D.K. & Sashidhar, R.B. A facile synthesis and characterization of Ag, Au and Pt nanoparticles using a natural hydrocolloid gum kondagogu (*Cochlospermum gossypium*). *Coll. Surf. B: Biointerfaces.*, 2011, **83**(2), 291-298. doi: 10.1016/j.colsurfb.2010.11.035.
  12. Kamal, S.S.K.; Sahoo, P.K.; Premkumar, M.; Vimala, J.; Ram, S. & Durai, L. A novel green chemical route for synthesis of silver nanoparticles using *Camellia Sinensis*. *Acta Chimi. Slov.*, 2010, **57**(4), 808-812.
  13. Yang, C.S.; Wang, X.; Lu, G. & Picinich, S.C. Cancer prevention by tea: Animal studies, molecular mechanisms and human relevance. *Nature Rev. Can.*, 2009, **9**(6), 429-439. doi:10.1038/nrc2641
  14. Satoh, E.; Ishii, T.; Shimizu, Y.; Sawamura, S.-I. & Nishimura, M. Black tea extract thearubigin fraction, counteract the effects of botulinum neurotoxins in mice. *Brit. J. Pharm.*, 2001, **132**(4), 797-978. doi:10.1038/sj.bjp.0703883
  15. Vanaja, M.; Rajeshkumar, S.; Paulkumar, K.; Gnanajobitha, G.; Malarkodi, C. & Annadurai, G. Kinetic study on green synthesis of silver nanoparticles using *Coleus aromaticus* leaf extract. *Adv. Appl. Sci. Res.*, 2013, **4**(3), 50-55.
  16. Al-Thabaiti, S.A.; Obaid, A.Y.; Hussain, S. & Khan, Z. Shape-directing role of cetyltrimethylammonium bromide on morphology of extracellular synthesis of silver nanoparticles. *Arab. J. Chem.*, 2015, **8**, 538-544. doi:10.1016/j.arabjc.2014.11.030

## ACKNOWLEDGEMENTS

Authors are thankful to Defence Research and Development Organisation, Ministry of Defence, Government of India for its support to carry out this work. We would like to thank the Director, DMRL, Hyderabad, for his keen interest in this work and also for permitting us to publish this work. We are thankful to Late Dr K. Chandrasekhar for his inspiration and guidance to carry out this work. Thanks are due to Dr M. Vijayakumar and Dr A.K. Singh, DMRL, Hyderabad for their support while carrying out the present work.

## CONTRIBUTORS

**Dr S.S. Kalyan Kamal** received his PhD (Materials Science) from Indian Institute of Technology, Kharagpur and is currently serving as a Scientist 'E' in Defence Metallurgical Research Laboratory, Hyderabad, India. His research interests are in the area of : Green chemical synthesis of nanoparticles, refractory materials and magnetic nanomaterials.

In the present work he has hypothesised and executed the experiments, collected and interpreted the data, and wrote the manuscript.

**Ms J. Vimala** is currently working as a Technical Officer in Defence Metallurgical Research Laboratory, Hyderabad, India. Her research interests are in the area of : Chemical characterisation of materials and green chemical synthesis of nanoparticles.

In the present work she has executed the experiments, collected and interpreted the data, and wrote the manuscript.

**Dr P.K. Sahoo** is currently serving as a Scientist 'D' in Defence Metallurgical Research Laboratory, Hyderabad, India. His research interests include : Synthesis of refractory based nanomaterials and nanocomposites.

He has recorded the FTIR spectrum and analysed the data.

**Dr P. Ghosal** is working as Scientist 'F' and Heading the Electron Microscopy Group in Defence Metallurgical Research Laboratory, Hyderabad, India. His specialisation is in the field of microstructural characterisation of nanomaterials.

In this work he assisted in collected, analysed and interpreted the SEM and TEM micrographs.

**Dr L. Durai** is working as Scientist 'F' and Heading the Analytical Chemistry Group, Defence Metallurgical Research Laboratory, Hyderabad, India. His research interests include: Chemical characterisation of materials and single crystal growth.

He is involved in writing and editing the manuscript and interpreting the results